Progress In Electromagnetics Research Letters, Vol. 95, 155–162, 2021

Conductivity Estimation by Characterization of the Anomalous Dispersion Region

Omar Siddiqui*

Abstract—Anomalous dispersion region is a resonance signature in the frequency response of resonators known as Lorentz resonators. It is identified by two consecutive slope reversals of the transmission phase response and a dip in the amplitude response. In this letter, we propose to exploit this unique resonant phase signature in characterization of the conductivity of solid and liquid material samples. The microwave resonator sensor consists of an open microstrip stub whose conductivity is designed to vary in response to an intruding sample. The transmission response of the resonator containing the material sample is measured using a vector network analyzer. The change of conductivity affects the Q-factor which can be detected by either the slope changes of the anomalous dispersive phase or the 3 dB bandwidth of the amplitude spectrum. The hypothesis is practically demonstrated by detecting resistive changes of a saline solution whose conductivity depends on the amounts of additive salt.

1. INTRODUCTION

Anomalous dispersion is an exciting physical phenomenon which was first discovered by Lord Raleigh while studying the resonances produced in mechanical oscillators [1]. Later, Sommerfield and Brillouin [2] analytically showed the existence of abnormal wave velocities in this highly dispersive and absorptive region. The experimental demonstration of negative group velocity helped clear misconceptions that historically surrounded the phenomenon [3–7]. The anomalous dispersion occurs naturally in materials in the THz range when constituent atoms resonate with the incoming light waves. The theoretical model which predicts this electromagnetic behavior was devised by Drude and Lorentz and hence is known as the Drude-Lorentz model [3, 8]. In the microwave spectrum, passive and active resonant circuits have been applied to mimic this atomic resonant behavior [6, 7, 9]. A simple RLC resonator configuration whose frequency response bears the anomalous dispersion region is given in Fig. 1 [6, 7, 10]. The associated transmission coefficient is marked by high amplitude absorption and rapid phase changes in the resonant region.

More recently, microwave sensors based on anomalous dispersion have demonstrated promising potential in the area of material detection [8, 10–12]. Compared to the traditional microwave sensing which relies on the detection of 3 dB amplitude bandwidth, the anomalous dispersive sensors work on the principle of phase-slope detection, which reduces the computational complexity, and work better in noisy environments. In these foundational works, the series RLC resonator has been chosen for dielectric characterization because of its simpler implementation as an open circuit stub [13]. Look again at Fig. 1 to observe the difference between the previously implemented dielectric sensing and the proposed conductivity characterization of this letter. The dielectric detection is based on introducing the sample in the cavity that *surrounds* the series RLC branch so that its capacitance 'C' is affected. The resulting shift of the resonant frequency and variation of the Q-factor correspond to the intruding dielectric parameters [8, 10–12]. Here, we propose to design a detection system in which the external

Received 4 September 2020, Accepted 28 December 2020, Scheduled 19 January 2021
* Corresponding author: Omar Siddiqui (omarsiddiqui2@gmail.com).
The author is with the College of Engineering, Taibah University, Madinah, Saudi Arabia.

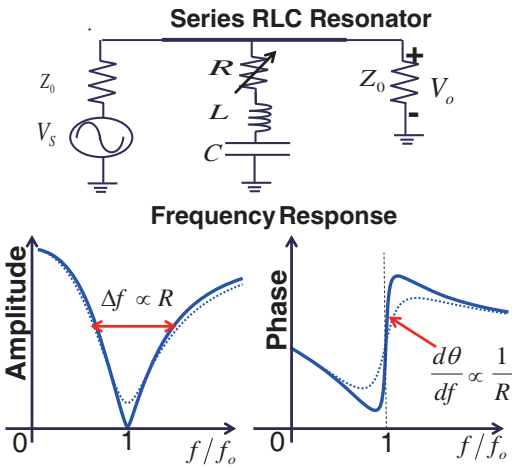

Figure 1. Series RLC and its transmission response. The anomalous dispersion region is identified by the dip in amplitude and reversals of the phase slopes. Effect of increase of resistance in the plots is shown by dotted lines.

conductive sample *modifies* the resistance 'R' of the series RLC resonator. As shown in Fig. 1, when the conductivity of a conductive material sample decreases, there is an increase in the series resistance leading to a wider amplitude response or an anomalous phase response with a smaller slope (see the dotted curve).

Practically, we design a conductivity-sensitive resonator by opening a small gap in the open-circuit stub in which saline solution of variable conductivity is introduced. The effects of conductivity on the resonator's Q-factor are characterized analytically and in an FR4-based microstrip structure in the frequency range of 1–1.5 GHz. We anticipate that the proposed conductivity sensor can be potentially used in various detection applications such as the detection of metallic particles in food [14, 15], sensing impurities in precious materials [16], and sea-water salinity detection [17].

2. ANALYTICAL FORMULATION

The series RLC resonator of Fig. 1 can be implemented in microstrip technology with an open-circuit quarterwave stub [13]. The quarterwave stub is well known for its narrowband characteristics and hence is widely implemented as a notch filter in antenna engineering [18]. From the sensing viewpoint, the notch type response translates to higher detection sensitivities [19]. Consider the microstrip implementation of the open stub structure and its circuit model in Fig. 2(a). The *complex* node voltages $\bar{V}_i$, $\bar{V}'$, and $\bar{V}_o$ are calculated by employing the Forward Transmission Matrix (FTM) method [20]. After applying the Kirchhoff's current equations on the three nodes, following simultaneous equations are obtained in the matrix form:

$$\begin{pmatrix} \bar{V}_i \\ \bar{V}' \\ \bar{V}_o \end{pmatrix} = \begin{pmatrix} \bar{P} & \bar{Q} & 0 \\ \bar{Q} & \bar{R} & \bar{Q} \\ 0 & \bar{Q} & \bar{P} \end{pmatrix}^{-1} \begin{pmatrix} \frac{V_s}{Z_o} \\ 0 \\ 0 \end{pmatrix} \tag{1}$$

where V_s is the source voltage, and Z_o is the characteristic impedance of the microwave system. P, Q, and R are complex frequency-dependent variables, defined as:

$$\bar{P} = -jY_{om} \cot \frac{\beta d}{2} + \frac{1}{Z_o} \tag{2}$$

$$\bar{Q} = jY_{om} \csc \frac{\beta d}{2} \tag{3}$$

$$\bar{R} = -2jY_{om} \cot \frac{\beta d}{2} + Y_{os} \tanh \bar{\gamma}_s L_s \tag{4}$$

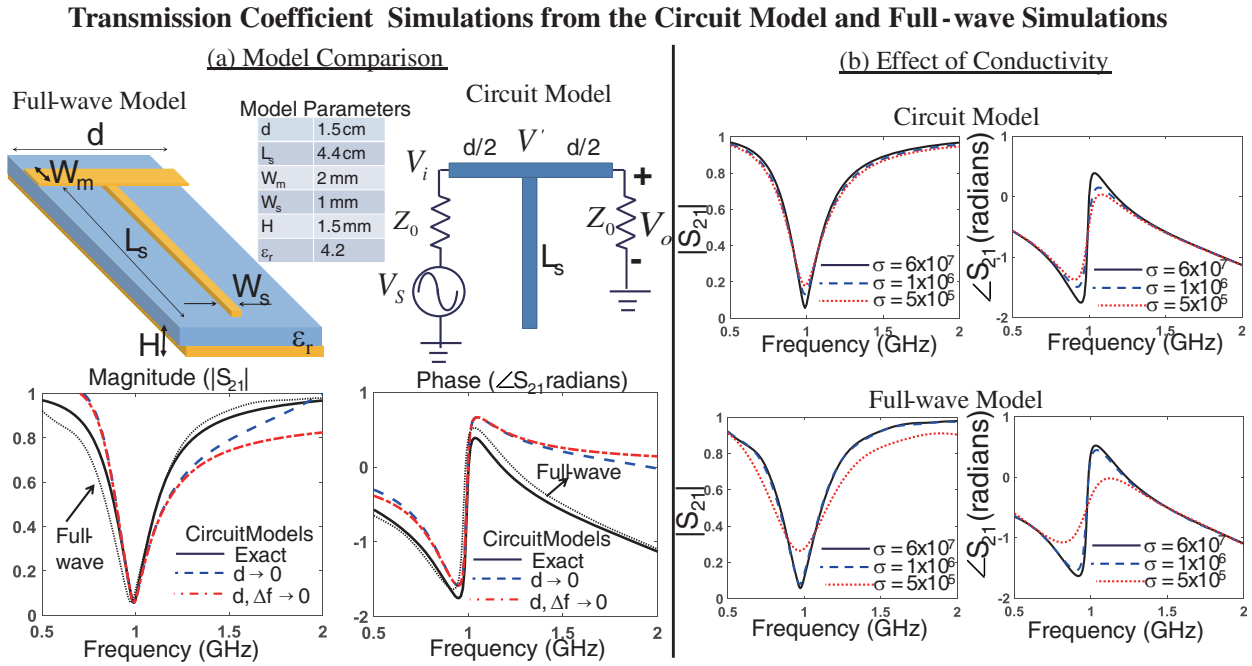

Figure 2. (a) Comparison of Amplitude and Phase Spectra of the Open-Stub resonator calculated from the circuit model and full-wave simulations. The parameters of the microstrip structure are given in the table. (b) The effect of change in conductivity on the bandwidth of the amplitude response and on the phase slope of the anomalous dispersion region.

where β, Z_{om} Y_{om}, and d are the phase constant, characteristic impedance, admittance, and length of the interconnecting transmission line, while $\bar{\gamma_s}$ and Y_{os} are the complex propagation constant and characteristic admittance of the open stub. The complex propagation constant is the sum of the attenuation and phase constants, i.e., $\alpha_s + j\beta_s$. Knowing the physical microstrip parameters outlined in Fig. 2(a), the characteristic impedances and phase constants can be determined from the well-known transmission line rules [13].

The magnitude and phase of the transmission coefficient are calculated from Eq. (1) and are shown in Fig. 2(a). The circuit model is also verified with the full-wave simulations using the electromagnetic simulator CST Microwave Studio [21]. As depicted in Fig. 2(a), the circuit and full-wave models demonstrate a close resemblance. The anomalous dispersion can be observed at $f_o = 0.99$ GHz at which the electrical length of the stub is approximately a quarter of the wavelength. Analytically, this frequency is given by:

$$f_o \cong \frac{c}{4\sqrt{\varepsilon_{es}}L_s}, \tag{5}$$

where ε_{es} is the effective relative permittivity. The output node voltage V_o can be further simplified by solving Eq. (1) with the assumption that the lengths of the transmission line segments connected to the open stub are small enough so that the phase βd is negligible. The output voltage can then be written as:

$$\bar{V_o} \approx \frac{1}{2 + (1 + j\beta d)(Z_o Y_{os} \tanh \bar{\gamma_s} L_s)} \tag{6}$$

Further approximation of the output voltage can be obtained in the spectral vicinity of the resonance by assuming $\Delta f = f - f_o$ in the above equation (i.e., when $\Delta f \to 0$),

$$\bar{V_o} \approx \frac{\alpha_s L_s + j\dfrac{\pi \Delta f}{2f_o}}{(2\alpha_s L_s + Z_o Y_{os}) + j\left(\beta d Z_o Y_{os} + \dfrac{\pi \Delta f}{f_o}\right)} \tag{7}$$

The approximate magnitude and phase spectra from the above two relations are also plotted along with the quantities obtained from the exact relation of Eq. (1) and the full-wave CST simulations in Fig. 2(a). The overlapping spectra close to the resonance in the anomalous dispersion region show the validity of the approximations assumed in Eqs. (6) and (7). From the point of view of conductivity sensing, the phase-slope of the anomalous dispersion region is particularly important as it corresponds to the losses in the structure [8, 10–12]. To quantify this underlying dependence, the phase angle obtained from the voltage Equation (7) is differentiated to find the slope. The resulting phase-slope is given by:

$$\frac{d}{df}(\angle \bar{V}_o) \approx \frac{Z_o Y_{os}}{\alpha_s L_s (2\alpha_s L_s + Z_o Y_{os})} \left(2\pi \alpha_s L_s \sqrt{\mu_o \varepsilon_{es}} d - \frac{\pi}{2f_o} \right) \tag{8}$$

It can be observed from Eq. (8) that an increase in the stub's loss corresponds to the decrease of the phase-slope. To demonstrate this correspondence, conductivity (σ) of the open circuit stub in the resonant circuit of Fig. 2(a) is varied, and the resulting magnitude and phase plots are depicted in Fig. 2(b). Looking at the magnitude plots, it can be seen that the decrease in conductivity leads to the broadening of the resonant curve or a reduction in the Q-factor of the resonator. Alternatively, the Q-factor reduction is accompanied by the obvious decrease in the phase slope, thus corroborating Eq. (8). Hence a detector based on anomalous dispersion provides an additional degree of freedom to estimate the structure's losses from the phase-slope, which are conventionally characterized by the bandwidth and Q-factor determination [19, 22–25]. In fact, this intimate relation between magnitude and phase is dictated by the well-known Kramers-Kronig relations and has been extensively discussed in the literature [2, 7, 26]. The phase detection has its own advantages such as noise immunity and computational simplicity which follows from the fact that the slope of the phase can be determined by knowing only two points on the phase curve. On the other hand, the amplitude method requires a complete analysis of the 3 dB bandwidth [8, 10–12].

3. DETECTION PRINCIPLE

The detection principle is based on Eq. (8) which relates the losses in the resonator to the phase-slope of the anomalous dispersion region. The attenuation constant in Eq. (8) can be calculated by the following microstrip rule:

$$\alpha_s = \frac{Y_s}{W_s} \sqrt{\frac{\pi f_o}{\sigma}} \tag{9}$$

A detection scheme which is sensitive to an external conductive sample can be obtained by introducing a small gap of 2 mm in the open stub, as depicted in Fig. 3(a). Consider a sample of volume $2 \times 1 \times 0.1\,\text{mm}^3$ having a dielectric constant 78 and a variable conductivity numerically placed in the gap. The magnitude and phase spectra from the CST full-wave solver are depicted in Figs. 3(b) and (c). Without any sample, there is a gap between the 3 cm and 1.2 cm stubs, and hence the structure resonates when the 3 mm stub becomes electrically equal to a quarter wavelength. From Eq. (5) and also indicated in Fig. 3 plots, this condition is satisfied around 1.42 GHz. The presence of a pure dielectric sample ($\sigma = 0$) with a large permittivity at the edge of the 3 cm stub effectively increases its electrical length, leading to a red-shift of the resonance to about 1.37 GHz. A slight increase in the conductivity ($\sigma = 5$) increases the resistive losses in the sample which leads to the broadening of the resonance dip and decrease of the phase-slope without any shift in the resonance, as depicted in Fig. 3. When conductivity is further increased, the sample starts acting like a resistor connecting the two open stubs. This phenomenon can be explained by magnetic field surface distributions given in Fig. 4. No current flow is observed in the shorter 1.2 cm microstrip segment for a non-conducting dielectric sample. For $\sigma = 50$, some current starts to reach the smaller segment, resulting in the increase of the effective stub length leading to a further red-shift of the resonance to 1.17 GHz and broadening of the resonance dip due to higher losses (see Fig. 3). For higher conductivity, the sample offers minimal resistance, and hence larger currents start flowing along the shorter segment. The resonant frequency in this case reaches its minimum value of 0.99 GHz. As observed in Figs. 3(b) and (c), the higher and lower conductivity samples in the conducting region are distinguished by their the Q-factor of the amplitude response or the slope of the phase response.

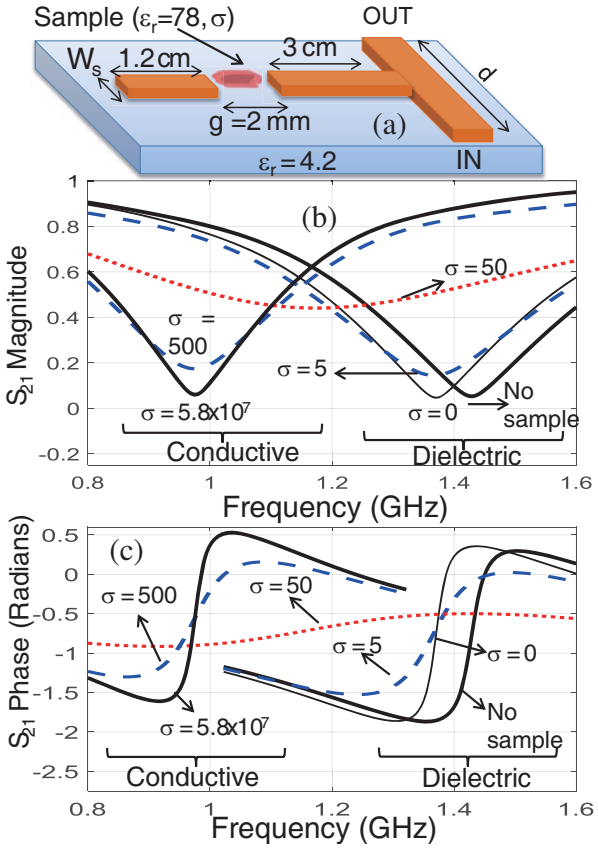

Figure 3. (a) Open circuit resonator sensor with a 2 mm gap where conductive sample is placed. (b) Transmission magnitudes for different samples (c) Transmission Phase showing the effect of change in conductivity.

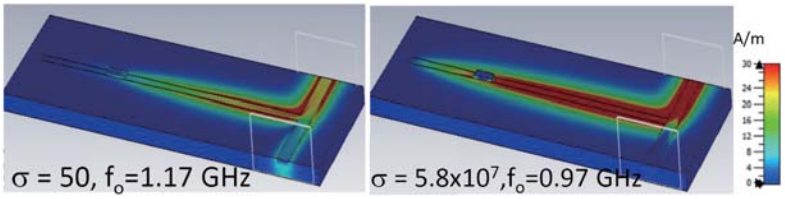

Figure 4. Magnetic field distributions showing the flow of current as the conductivity of the gap material is increased. For a high conductive sample in the gap, the current flows throughout the two microstrip segments

4. EXPERIMENTAL RESULTS

The simulation scenario presented in Fig. 3 can be implemented practically by introducing a conductive saline solution in the open stub gap. The microstrip open stub structure of Fig. 2 is printed on an FR4 substrate using photolithographic fabrication process. The circuit prototype and the S_{21} measurement setup with Anritsu's MS2026C vector network analyzer (VNA) are depicted in Figs. 5(a) and (b). A conductive solution is prepared by adding measured amounts of table salt to a 170 ml cup of tap water, as depicted in Fig. 5(c). The sample conductive solution is placed in the open stub gap by using a dropper, as shown in Fig. 5(d), and transmission coefficient is measured by the VNA. The measured amplitude and phase of the transmission coefficient are given in Fig. 6. By comparing Fig. 4 and Fig. 6, it can be observed that simulated and measured resonant circuits (with no sample) resonate at almost

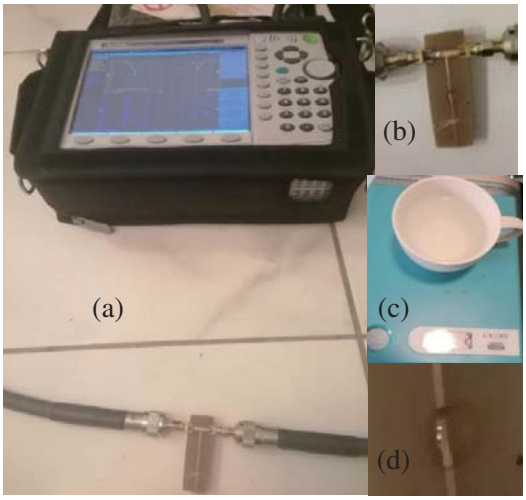

Figure 5. (a) The S-parameter measurement set-up to characterize conductivity using Anritsu's VNA. (b) The open-circuit stub resonator with a gap to put the conductive sample. (c) Saline solution which is prepared by dissolving measured amounts of salt in 170 ml water. (d) The saline water droplet on the conductivity sensor. The metallic coin sample is placed for detection.

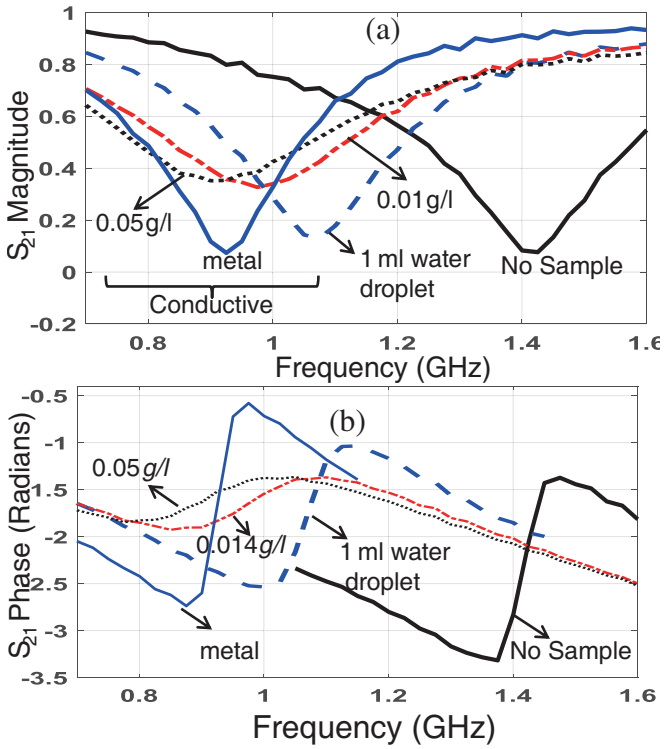

Figure 6. Experimental transmission coefficients obtained from VNA measurement showing. (a) The change in amplitude response with different samples. (b) The change in phase response.

the same resonant frequencies. The slope of the measured anomalous phase is, however, smaller due to some of the factors such as connector losses and fabrication imperfections not taken into account in the full-wave simulations. When a 1 ml droplet of tap water is placed in the open stub gap, a larger red-shift of the resonance is observed than the similar scenario in Fig. 5. The larger shift can

be attributed to the fact that the tap water contains some ingredients such as chlorine and minerals that were not accounted for in the CST simulations. As expected, the addition of salt makes the water conductive, and the sample enters the conductive region, as observed in the previous section. The 0.05 g/l saline sample has enough conductivity to excite the currents in the 1.2 cm microstrip segment, and the resonant frequency approaches that of the highly conductive metal sample, as shown in Fig. 6. However, the higher Q-factor (indicated by larger phase-slope and narrower bandwidth) differentiates the pure metal and saline samples. The experiment performed here shows the relationship between the sample's conductivity and the resonator's Q-factor in a qualitative way. For the determination of conductivity (qualitative analysis), a calibration process is required which involves extensive testing with known conductivity samples. This is needed for commercial prototyping of any sensor and will be a topic of a future publication.

Finally, a discussion regarding the difference between the proposed resonator-based detection and the existing metallic detectors is in order. Most of the existing conductivity determination methods are based on harmonically balanced inductive coil and involve very low frequency beat signals. In the presence of a conductive sample, the harmonic balance is disturbed which is identified by the change in the tone signal [14, 15]. A very high conductivity sample is needed to produce a strong beat difference to detect the presence of metal. Signal processing methods in combination with statistical analysis have been used to identify the small changes in conductivity [15]. The proposed method, on the other hand, is based on detecting the resonance shift and Q-factor of a highly dispersive Lorentz resonator. Since the detection is done in a very narrowband spectrum, the method is highly sensitive to small changes in conductivity, as observed in Fig. 6.

5. CONCLUSION

A sensing method to estimate the conductivity of materials based on the characterization of anomalous dispersion region is proposed. The microwave sensor consists of an open circuit stub with a small gap which houses the conductive sample. The variation of the material's conductivity changes the resistance of the open stub which leads to an increase or decrease of the sensor's Q-factor. The Q-factor changes are calculated from the bandwidth of the amplitude spectrum or the slope of the anomalous dispersion region. We derive analytical equations of transmission coefficients and show the dependence conductivity on the parameters of the anomalous dispersion region. A correspondence between the circuit analysis and full-wave simulations is shown. The sensing method is practically demonstrated by introducing a saline solution in the detection scheme. When the salinity is increased, the variation of Q-factor is noted in both full-wave solution and experiment. The characterization of anomalous dispersion region is particularly interesting because the distinct phase signature provides another degree of freedom to the traditional amplitude sensing, thereby reducing the ambiguity in the detection. The sensor can be potentially applied in impure metal detection, water salinity and in food industry.

REFERENCES

1. Dogariu, A., A. Kuzmich, and L. Wang, "Transparent anomalous dispersion and superluminal light-pulse propagation at a negative group velocity," *Physical Review A*, Vol. 63, No. 5, 053806, 2001.
2. Brillouin, L., *Wave Propagation and Group Velocity*, Vol. 8, Academic Press, 2013.
3. Jackson, J. D., *Classical Electrodynamics*, John Wiley & Sons, 2007.
4. Bolda, E. L., J. C. Garrison, and R. Y. Chiao, "Optical pulse propagation at negative group velocities due to a nearby gain line," *Physical Review A*, Vol. 49, No. 4, 2938, 1994.
5. Wang, L., A. Kuzmich, and A. Dogariu, "Gain-assisted superluminal light propagation," *Nature*, Vol. 406, No. 6793, 277–279, 2000.
6. Siddiqui, O. F., S. J. Erickson, G. V. Eleftheriades, and M. Mojahedi, "Time-domain measurement of negative group delay in negative-refractive-index transmission-line metamaterials," *IEEE Transactions on Microwave Theory and Techniques*, Vol. 52, No. 5, 1449–1454, 2004.

7. Siddiqui, O. F., M. Mojahedi, and G. V. Eleftheriades, "Periodically loaded transmission line with effective negative refractive index and negative group velocity," *IEEE Transactions on Antennas and Propagation*, Vol. 51, No. 10, 2619–2625, 2003.
8. Siddiqui, O. F., R. Ramzan, M. Amin, M. Omar, and N. Bastaki, "Lorentz reflect-phase detector for moisture and dielectric sensing," *IEEE Sensors Journal*, Vol. 18, No. 22, 9236–9242, 2018.
9. Solli, D., R. Chiao, and J. Hickmann, "Superluminal effects and negative group delays in electronics, and their applications," *Physical Review E*, Vol. 66, No. 5, 056601, 2002.
10. Siddiqui, O., R. Ramzan, M. Omar, and M. Amin, "Phase sensinga novel material characterization method," *2017 International Conference on Electrical and Computing Technologies and Applications (ICECTA)*, 1–4, IEEE, 2017.
11. Ramzan, R., O. F. Siddiqui, M. W. Arshad, and O. M. Ramahi, "A complex permittivity extraction method based on anomalous dispersion," *IEEE Transactions on Microwave Theory and Techniques*, Vol. 64, No. 11, 3787–3796, Nov. 2016.
12. Siddiqui, O., R. Ramzan, M. Amin, and O. M. Ramahi, "A non-invasive phase sensor for permittivity and moisture estimation based on anomalous dispersion," *Scientific Reports*, Vol. 6, Jun. 2016.
13. Pozar, D., *Microwave Engineering*, John Wiley & Sons, 2005.
14. Kharangate, L. S., N. Guinde, and A. Tamba, "A novel approach for metal detection in food using curve fitting technique," *2017 2nd IEEE International Conference on Recent Trends in Electronics, Information & Communication Technology (RTEICT)*, 1867–1871, IEEE, 2017.
15. Haimovich, H., D. Marelli, and D. Sarlinga, "A signal processing method for metal detection sensitivity improvement in balance-coil metal detectors for food products," *2020 IEEE International Conference on Industrial Technology (ICIT)*, 645–651, IEEE, 2020.
16. Nor, F. M., A. R. Tamuri, and A. K. Ismail, "Fake gold: Gold purity measurement using non destructive method," *International Journal of Engineering & Technology*, Vol. 8, No. 1.1, 165–172, 2019.
17. Robinson, S. and R. Nakkeeran, "Photonic crystal based sensor for sensing the salinity of seawater," *IEEE-International Conference On Advances In Engineering, Science And Management (ICAESM-2012)*, 495–499, IEEE, 2012.
18. Hong, J.-S. G. and M. J. Lancaster, *Microstrip Filters for RF/Microwave Applications*, Vol. 167, John Wiley & Sons, 2004.
19. Chen, L.-F., C. Ong, C. Neo, V. V. Varadan, and V. K. Varadan, *Microwave Electronics: Measurement and Materials Characterization*, John Wiley & Sons, 2004.
20. Siddiqui, O., "The forward transmission matrix method for S-parameter analysis of microwave circuits and their metamaterial counterparts," *Progress In Electromagnetics Research B*, Vol. 66, 123–141, 2016.
21. Systems, D., Cst microwave studio, https://www.3ds.com/products-services/simulia/products/cst-studio-suite/.
22. Kobayashi, Y. and M. Katoh, "Microwave measurement of dielectric properties of low-loss materials by the dielectric rod resonator method," *IEEE Transactions on Microwave Theory and Techniques*, Vol. 63, 2466–2488, Apr. 1985.
23. Dube, D., M. T. Lanagan, J. H. Kim, and S. J. Jang, "Dielectric measurements on substrate materials at microwave frequencies using a cavity perturbation technique," *Journal of Applied Physics*, Vol. 63, 2466–2488, Apr. 1988.
24. Santra, M. and K. U. Limaye, "Estimation of complex permittivity of arbitrary shape and size dielectric samples using cavity measurement technique at microwave frequencies," *IEEE Transactions on Microwave Theory and Techniques*, Vol. 53, 718–722, Feb. 2005.
25. Sheen, J., "Study of microwave dielectric properties measurements by various resonance techniques," *Measurement*, Vol. 37, 123–130, Dec. 2005.
26. Kronig, R. D. L., "On the theory of the dispersion of x-rays," *J. Opt. Soc. Am.*, Vol. 12, 547–557, 1926.